Bimodal behaviour observed by quasi-elastic light scattering in the cross-over region from Θ to critical temperature

Masato Takahashi and Takuhei Nose*
Department of Polymer Chemistry, Tokyo Institute of Technology, Ookayama, Meguro-ku, Tokyo 152, Japan
(Received 24 September 1985; revised 14 November 1985)

The dynamic behaviour of a polystyrene ($M_w = 2.89 \times 10^6$)–cyclohexane solution was investigated by quasi-elastic light scattering in the cross-over region from Θ to critical temperature. The following results were obtained. (1) The time-correlation function of concentration fluctuations showed bimodal decay in the semidilute region (at concentrations $C \geqslant 3.32 \times 10^{-2}$ g polystyrene/g solution. (2) The linewidth Γ_f for the fast mode had k^2-dependence, while Γ_s for the slow mode exhibited an anomalous angular dependence. As the temperature T approached the critical temperature T_c, however, Γ_s tended to show the k^2-dependence too. (3) In the critical solution, temperature dependences of Γ_s and Γ_f were described by $\Gamma_s \propto t^{0.5}$ and $\Gamma_f \propto t^{-1}$ ($t \equiv |T - T_c|/T_c$), respectively, suggesting that Γ_s and Γ_f correspond to the critical and background parts of average linewidth. As the temperature approached T_c, the amplitude of the slow mode relative to that of the fast mode increased very sharply, and as a result the correlation function approached becoming unimodal. (4) At the Θ-temperature, Γ_f increased with increasing concentration, whereas Γ_s decreased. These concentration dependences were qualitatively, but not quantitatively, consistent with the predictions for the gel-mode and the reptation motion, respectively.

(Keywords: quasi-elastic light scattering; semidilute polymer solution; critical phenomena; dynamic properties)

INTRODUCTION

In our previous study[1], we measured dynamic light scattering from binary critical solutions of polystyrene (PS)–methylcyclohexane with molecular weight ranging from 1.75×10^4 to 1.26×10^6 in the temperature region from Θ to critical point. It was found that the average linewidth $\bar{\Gamma}$ for higher molecular-weight samples did not follow the mode–mode coupling theory of Kawasaki[2]

$$\Gamma_C/k^3 = \frac{k_B T}{8\pi\eta^*}(k\xi)^{-3}[1 + (k\xi)^3 + \{(k\xi)^3 - (k\xi)^{-1}\}\arctan(k\xi)] \qquad (1)$$

including large background Γ_B, where Γ_C is the critical part of $\bar{\Gamma}(=\Gamma_B + \Gamma_C)$, k the magnitude of the scattering wavevector, defined by $k = (4\pi/\lambda)\sin(\theta/2)$ with the wavelength λ in the medium and the scattering angle θ, k_B the Boltzmann constant, T the absolute temperature, η^* the viscosity of solution, and ξ the correlation length. The deviation from theory became more appreciable as the molecular weight increased. Temperature dependence of critical and background parts of $\bar{\Gamma}$ in the hydrodynamic region was described by

$$\bar{\Gamma} \simeq \Gamma_C + \Gamma_B \simeq \Gamma_{C0}t^{\nu} + \Gamma_{B0}t^{\gamma} \qquad (2)$$

where Γ_{C0} and Γ_{B0} are constants, $t \equiv |T - T_c|/T_c$, and ν and γ are the critical exponents for the correlation length and isothermal osmotic compressibility, respectively. Histogram analysis showed that the fast and slow decay modes were involved in the correlation function $g^{(1)}(\tau)$ for molecular weights $M_w \geqslant 4.22 \times 10^5$. It was suggested that this bimodal decay may be closely related to the large background and the deviation from the Kawasaki theory. However, the contribution of the fast mode to $g^{(1)}(\tau)$ was so small, owing to relatively low values of the molecular weight used, that no quantitative analysis of the fast mode was made.

Such a bimodal decay in the correlation function has already been found for semidilute polymer solutions in good[3-10] and theta solvents [10-13] by many investigators. Usually, $g^{(1)}(\tau)$ can be approximated by the sum of two exponential decays:

$$g^{(1)}(\tau) = A_f\exp(-\Gamma_f\tau) + A_s\exp(-\Gamma_s\tau) \qquad (3)$$

where Γ_f and Γ_s are the line-widths of fast and slow modes with amplitudes A_f and A_s, respectively. The magnitudes of Γ_s and A_s/A_f are markedly dependent upon molecular weight, solvent quality, concentration, and k. The fast and slow modes have often been assigned to the gel-mode and the mode of motions associated with the reptation, respectively. To examine these assignments, Brown *et al.*[7,10] have compared the values of Γ_f and Γ_s with the results obtained by other experimental methods such as classical gradient diffusion, sedimentation, pulsed-field gradient n.m.r., and forced Rayleigh light scattering.

The experiments for semidilute theta solutions have been made mostly at and above the Θ-temperature. Studies below the Θ-temperature, however, have only been made by Munch *et al.*[14] and the authors[1], to the best of our knowledge.

In this study, the bimodal behaviour of concentration fluctuations in the temperature region from Θ to critical

---

* To whom all correspondence should be addressed.

0032-3861/86/071071-07$03.00

point has been investigated by dynamic light scattering for PS in cyclohexane with higher molecular weight than in the previous study.

EXPERIMENTAL

Samples

The PS sample was a Toyo Soda Co. product with molecular weight 2.89×10^6 ($M_w/M_n < 1.09$). Cyclohexane of spectroscopic grade was dehydrated on calcium hydride and purified by fractional distillation.

Critical concentration C_c and temperature T_c were determined by the method described previously[1], and were found to be $C_c = 3.49 \times 10^{-2}$ g PS/g solution and $T_c = 303.53$ K. 2-Butanone solution with concentration around 3.5×10^{-2} g solute/g solution was filtered through a Millipore filter (FSLW01300, pore size: 3 μm), to remove dust particles, into a light-scattering cell with diameter 10 mm (or 5 mm for the critical concentration). Then, the 2-butanone was completely removed by evaporation under vacuum at about 60°C, followed by adding cyclohexane into the cell through a Millipore filter (FGLP01300, pore size: 0.2 μm) to make a solution of the desired concentration. The concentration ranged from 4.51×10^{-3} to 1.46×10^{-1} g PS/g solution.

Apparatus

Static and dynamic light scattering was measured by two light-scattering apparatus. One was the previously reported one[1] with an argon-ion laser (Nippon Electric Co. model GLG 3200) operating at the wavelength $\lambda_0 = 488$ nm and a 48-channel Malvern digital correlator K7023. The other was a Malvern photometer (PCS100SM) with a He–Ne laser (Spectra-Physics Stabilite, model 1248) ($\lambda_0 = 633$ nm) and a Malvern digital correlator K7027. Temperature was controlled to within ± 0.01°C and ± 0.1°C for the two apparatus, respectively.

Data analysis

The correlation length, ξ, and the intensity of scattered light at $k = 0$, I_0, were determined from the angular dependence of scattered light intensity by the method used previously[1].

The normalized correlation function $g^{(1)}(\tau)$ of the scattered electric field was computed from a measured photocount autocorrelation function $G^{(2)}(\tau)$ by the equation

$$G^{(2)}(\tau) = A(1 + \beta |g^{(1)}(\tau)|^2)$$

where A is the background, and β is an unknown parameter in the data-fitting procedure.

The correlation function $g^{(1)}(\tau)$ for the solutions with concentration $C \leqslant 1.85 \times 10^{-2}$ g per gram showed a unimodal decay, which was analysed by the method of cumulants[15] to obtain the average linewidth $\bar{\Gamma}$.

In the semidilute solutions ($C \geqslant 3.32 \times 10^{-2}$ g per gram), the correlation function $g^{(1)}(\tau)$ exhibited a bimodal decay so that the data for $g^{(1)}(\tau)$ with a wide range of timescale were necessary for the analysis. In the measurements by K7023, the correlation function $g^{(1)}(\tau)$ over three orders of timescale was obtained from the data with several different sample times by adjusting the normalization factor, while the correlator K7027 measured the autocorrelation function $G^{(2)}(\tau)$ over four orders of timescale by one run with a logarithmic progression of delay times. The linewidth and amplitude for slow and fast decay modes, Γ_s, Γ_f, A_s and A_f, were evaluated by a nonlinear least squares fit of $g^{(1)}(\tau)$ to equation (3).

RESULTS AND DISCUSSION

Profile of correlation function

Figure 1 shows the time-correlation functions for $C = 4.51 \times 10^{-3}$, 3.32×10^{-2} and 0.146 g per gram at $T = 307.65$ K (the Θ-temperature). The linewidth distribution becomes broader with increasing concentration, and an appreciable separation of the two modes was observed at $C \geqslant 3.32 \times 10^{-2} \approx C_c$.

Figure 2 represents angular dependence of $g^{(1)}(\tau)$, where two correlation functions obtained at different scattered angles were plotted against $\tau \sin^2(\theta/2)$ with a double logarithmic scale. The two decay curves superimpose well on each other at small τ's in contrast with the branching of long-time tails, suggesting non-k^2-dependence of Γ_s. In fact, as shown in *Figures 3* and *4*, Γ_f has k^2-dependence, while Γ_s exhibits an anomalous angular dependence, appearing to have a finite value at $k = 0$. But, as the temperature approaches T_c, the plot of Γ_s vs. $\sin^2(\theta/2)$ tends to intersect the ordinate at a point nearer the origin, i.e. the angular dependence approaches k^2. Very recently, in semidilute solutions at the Θ-temperature, Amis *et al.*[12] and Brown *et al.*[10] observed k^2-dependence for both Γ_f and Γ_s, whereas Adam *et al.*[13] found that Γ_s was independent of k, although Γ_f obeyed k^2-dependence in the region of $k\xi < 1/3$. Since the molecular weights used by Amis *et al.* ($M_w = 1.79 \times 10^5$–1.05×10^6) and Brown *et al.* ($M_w = 9.3 \times 10^4$–9.3×10^5) were smaller than those used

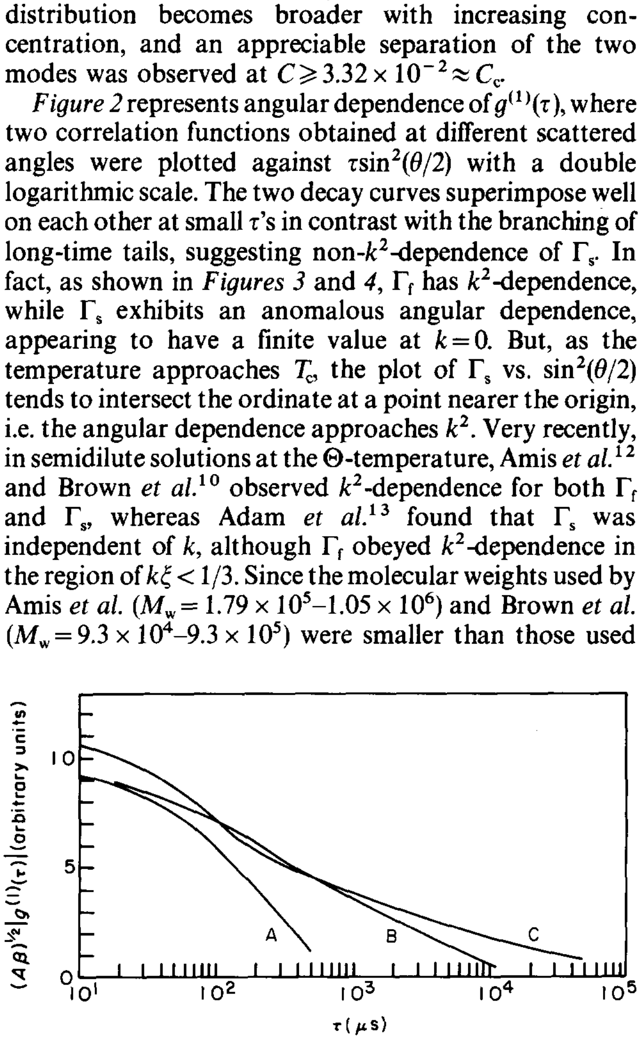

Figure 1 Correlation function $g^{(1)}(\tau)$ for $C = 4.51 \times 10^{-3}$ g per gram (A), 3.32×10^{-2} (B), and 0.146 (C) measured at $T = 307.65$ K (the Θ-temperature), $\theta = 90°$, and $\lambda_0 = 488$ nm

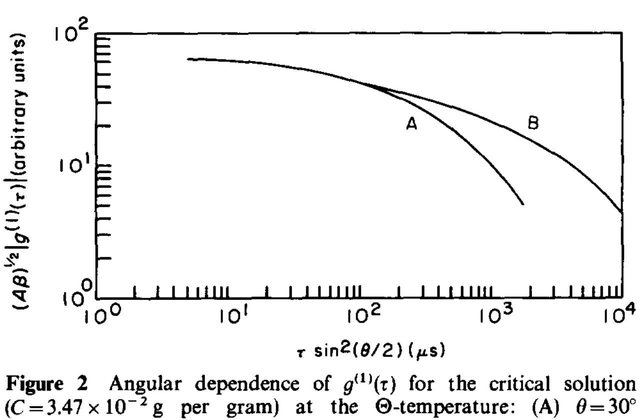

Figure 2 Angular dependence of $g^{(1)}(\tau)$ for the critical solution ($C = 3.47 \times 10^{-2}$ g per gram) at the Θ-temperature: (A) $\theta = 30°$ ($k = 9.48 \times 10^{-3}$ nm^{-1}); (B) $\theta = 150°$ ($k = 3.54 \times 10^{-2}$ nm^{-1})

by Adam *et al.* ($M_w = 3.84 \times 10^6$–2.06×10^7), the molecular-weight difference may be responsible for the difference in the angular dependence of Γ_s. The molecular weight used in the present work is intermediate between those used in the experiments quoted, so that our result may be the cross-over behaviour from k^2-dependence for lower molecular weights to k-independence for higher ones.

Figure 5 represents angular dependence of A_s/A_f, indicating that the ratio A_s/A_f increases with decreasing k. This fact suggests that the slow mode corresponds to the concentration fluctuations with a spatially larger scale than the fast mode. This tendency in the k-dependence of A_f/A_s becomes more pronounced as the temperature approaches T_c.

Dynamic properties of the critical solution

The values of Γ_s and Γ_f for the critical solution ($C = 3.47 \times 10^{-2}$ g per gram) at $\theta = 90°$ and $\lambda_0 = 488$ nm are plotted against t in *Figure 6* along with the t-value at $k\xi = 1$. Temperature dependence of Γ_s in the hydrodynamic region ($k\xi < 1$) can be approximated by the power law

$$\Gamma_s \propto t^b \qquad (4)$$

with the value of the exponent b being around 0.5. Although the accuracy of Γ_f is not so good as that of Γ_s, owing to a high sensitivity of Γ_f-evaluation to the choice of the sample time, Γ_f appears to have a temperature dependence stronger than Γ_s in the hydrodynamic region.

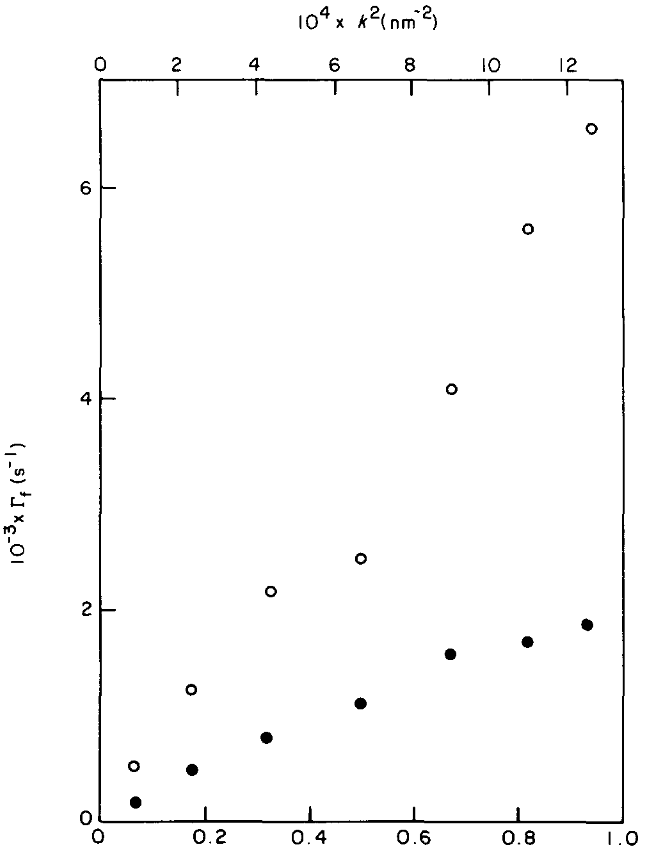

Figure 3 Angular dependence of Γ_f for the critical solution at the Θ-temperature (○) and 305.15 K (●)

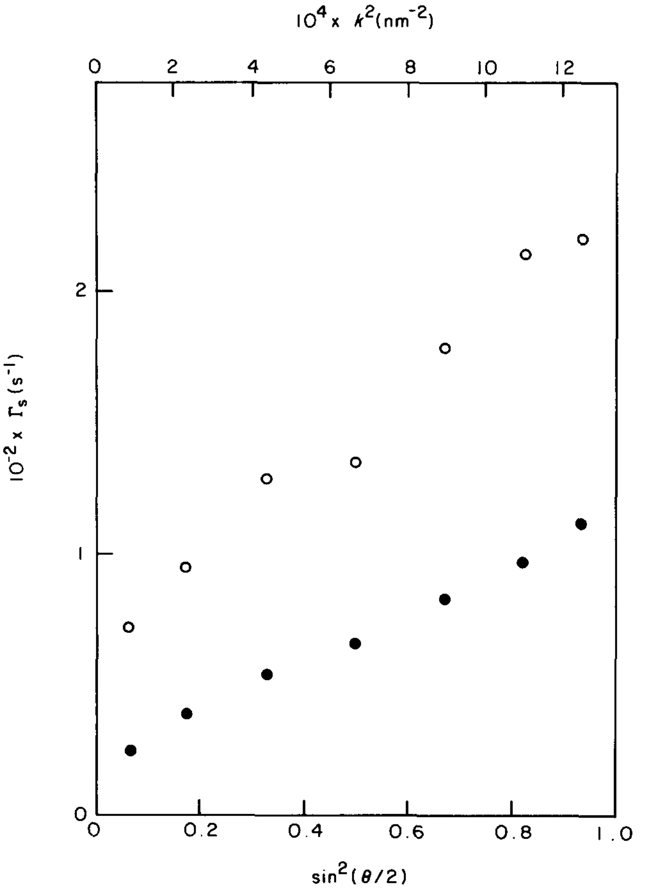

Figure 4 Angular dependence of Γ_s for the critical solution at the Θ-temperature (○) and 305.15 K (●)

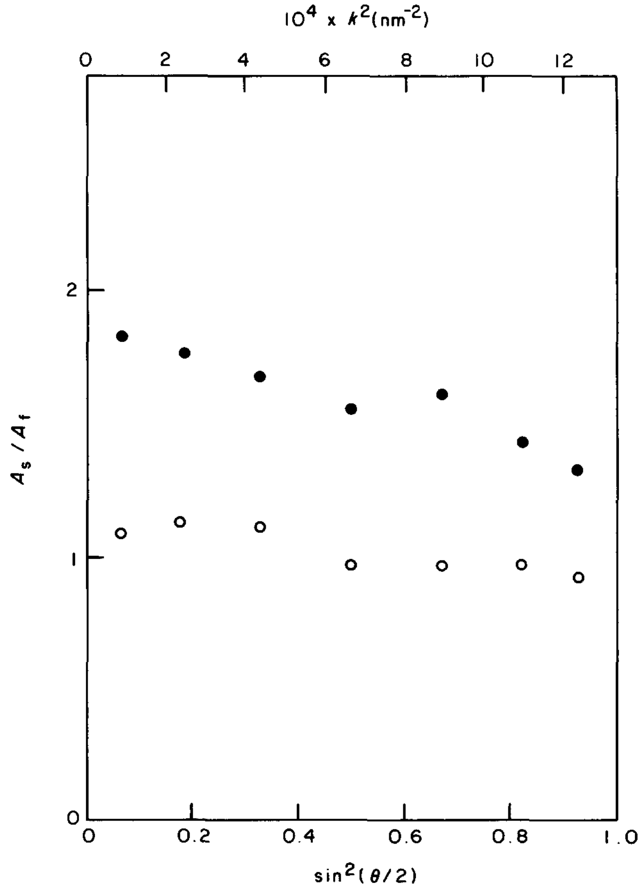

Figure 5 Angular dependence of A_s/A_f for the critical solution at the Θ-temperature (○) and 305.15 K (●)

These t-dependences of Γ_s and Γ_f in $k\xi<1$ seem to correspond to those of ξ^{-1} and $(I_0/T)^{-1}$, respectively, suggesting that $\Gamma_s \propto \xi^{-1}$ and that $\Gamma_f \propto T/I_0$. Namely, as shown in *Figures 7* and *8*, t-dependences of ξ and I_0/T can be expressed as the power laws

$$\xi = 22.6 t^{-\nu} \text{Å} \qquad (5)$$

and

$$I_0/T \propto t^{-\gamma} \qquad (6)$$

with the critical exponents $\nu = 0.50$ and $\gamma = 1.05$. These exponents ν and γ are comparable to the exponent b and the slope of log Γ_f vs. log t plotted at $k\xi < 1$, respectively. (The exponents ν and γ are rather close to the classical ones[16].)

The ratio A_s/A_f is plotted against T in *Figure 9*. As the temperature approaches T_c, the ratio increases very rapidly so that the slow mode becomes dominant, and consequently the correlation function approaches a single exponential decay, as shown in *Figure 10*. Above the Θ-temperature, it has been found that A_s/A_f increases as solvent quality becomes poorer[7,10,11]. The present result

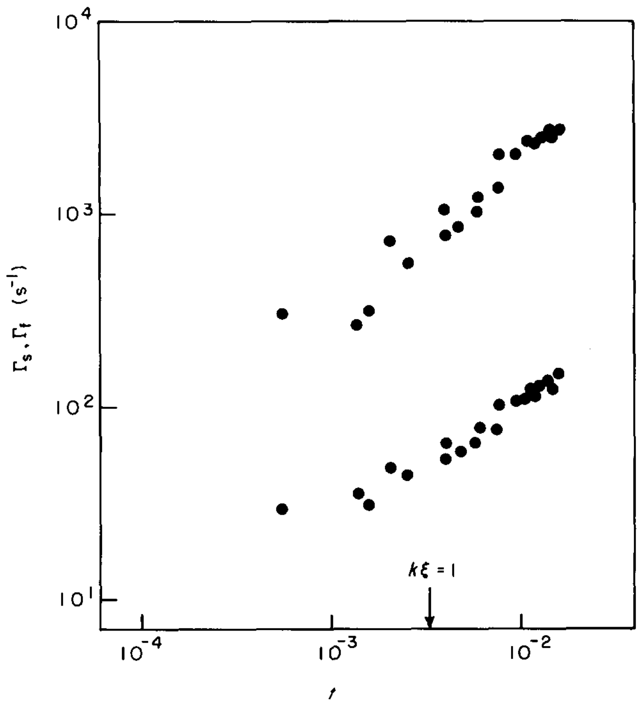

Figure 6 Temperature dependence of Γ_f and Γ_s for the critical solution at $\theta = 90°$ and $\lambda_0 = 488$ nm

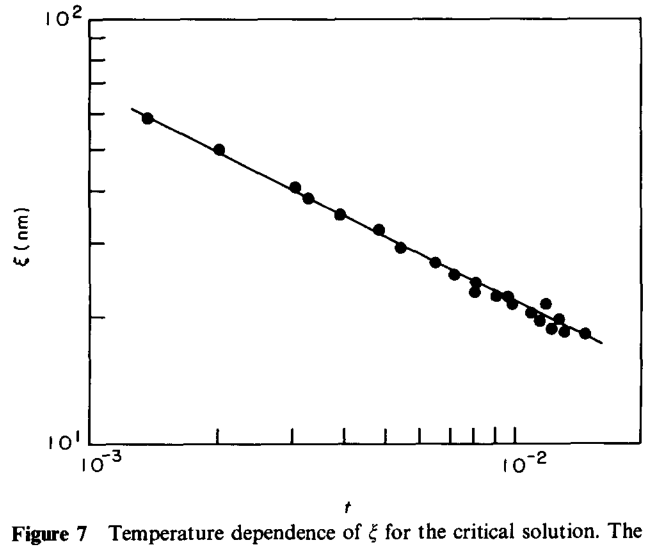

Figure 7 Temperature dependence of ξ for the critical solution. The solid line was obtained by a least-squares fit (equation (5))

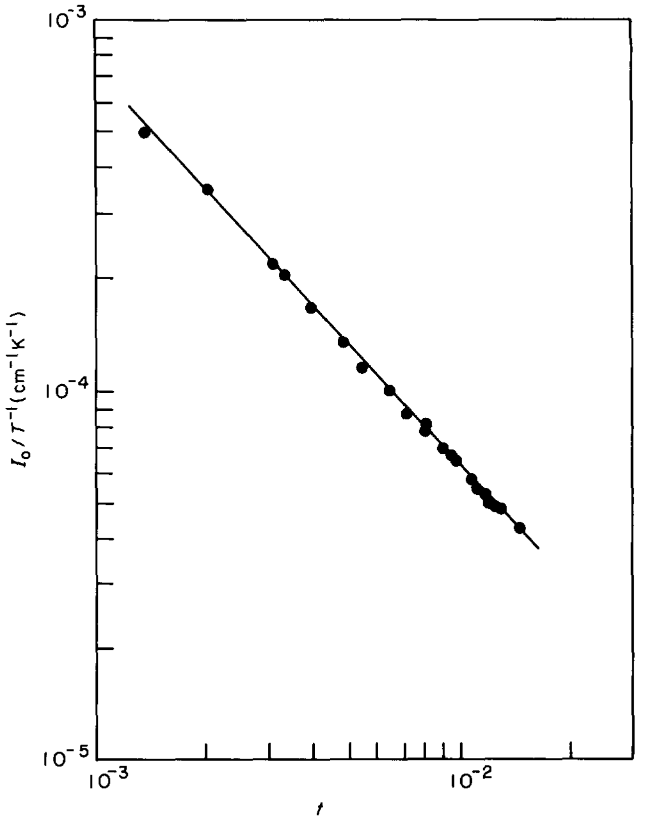

Figure 8 Temperature dependence of I_0/T for the critical solution. The solid line was obtained by a least-squares fit (equation (6))

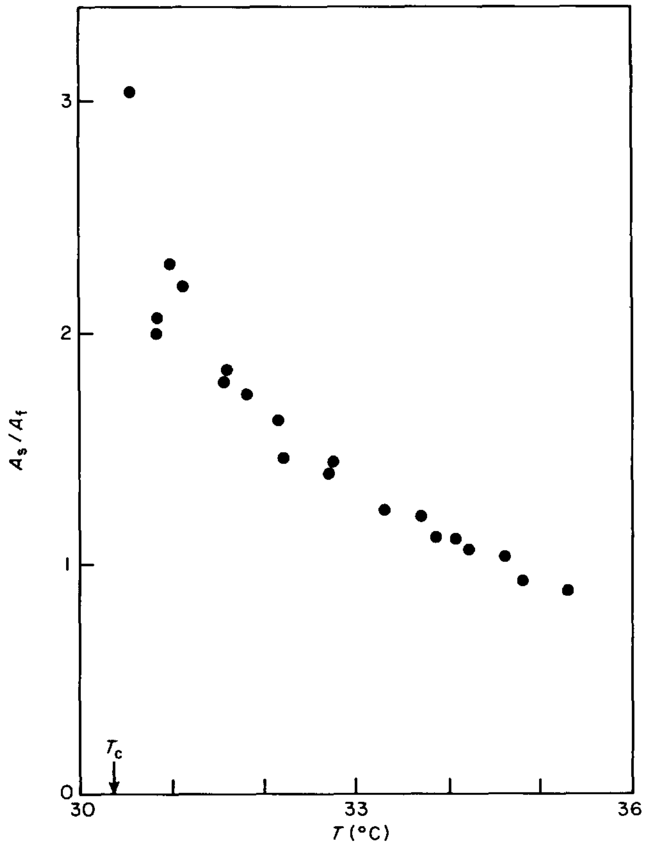

Figure 9 Temperature dependence of A_s/A_f for the critical solution at $\theta = 90°$ and $\lambda_0 = 488$ nm

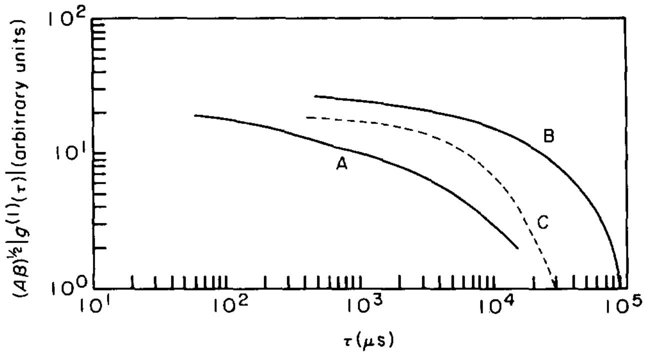

Figure 10 Temperature dependence of $g^{(1)}(\tau)$ ($\theta=90°$ and $\lambda_0=488$ nm) for the critical solution at the Θ-temperature (A) and 303.7 K (B). The broken curve (C) represents the single-exponential decay function for reference

has verified that this tendency also holds below the Θ-temperature.

Reminding ourselves of the previous result of equation (2), the findings that $\Gamma_s \propto 1/\xi$, and that $\Gamma_f \propto T/I_0$ seem to show that the slow and fast modes correspond to the critical and background parts, respectively. This assignment is supported by the rapid growth of A_s/A_f near T_c and also by the increment of A_s/A_f with decreasing scattering angle, because, if this is so, the slow mode is ascribed to concentration fluctuations with longer wavelength.

In general, the correlation function $g^{(1)}(\tau)$ near the critical temperature exhibits a single exponential decay with the linewidth Γ being composed of the critical part Γ_C and the background part Γ_B (refs. 17 and 18)

$$\Gamma = \Gamma_C + \Gamma_B \tag{7}$$

For polymer solutions Γ_C and Γ_B, in the hydrodynamic region, is given by

$$\Gamma_C/k^2 = \frac{k_B T}{2^{1/2}\pi\eta^* N^{1/4} a}\left(\frac{\chi_c-\chi}{\chi_c}\right)^{1/2} \propto t^{1/2} \tag{8}$$

and

$$\Gamma_B/k^2 \sim \frac{k_B T}{\eta_s a}\left(\frac{\chi_c-\chi}{\chi_c}\right) \propto t \tag{9}$$

as derived in the Appendix, where N is the polymeric index, χ the Flory–Huggins interaction parameter, a the segment length, and η_s the solvent viscosity.

Temperature dependences of Γ_C and Γ_B given by equations (8) and (9) correspond to those in equation (2). The exponents 1/2 and 1 in equations (8) and (9) are the classical critical exponents for ν and γ, respectively. As generally expected, the difference between the values of these exponents results in dominance of the critical part Γ_C near the critical point.

The ratio Γ_B/Γ_C is derived from equations (8) and (9) as

$$\Gamma_B/\Gamma_C \sim N^{1/4}\left(\frac{\chi_c-\chi}{\chi_c}\right)^{1/2} \sim N^{1/4} t^{1/2} \tag{10}$$

in the hydrodynamic region, indicating that the relative value of Γ_B to that of Γ_C increases with increasing N and t. The temperature range in this experiment is not close to T_c so that the correlation function exhibits a bimodal decay because of the comparable contributions of critical and background fluctuations to the correlation function. But, as the temperature becomes much closer to T_c, the ratio Γ_B/Γ_C will become smaller and the single exponential decay will be observed. In the previous paper, we reported that the bimodal behaviour becomes more appreciable with increasing molecular weight. This fact can be readily understood from equation (10). It should be noted that a temperature T', at which the two modes are comparable, changes with N as

$$\frac{T'-T_c}{T_c} \sim \left(\frac{\chi_c-\chi'}{\chi_c}\right) \sim N^{-1/2} \tag{11}$$

(from equation (10)), i.e. the critical region ($|T-T_c|<|T'-T_c|$) becomes narrower with increasing molecular weight, which agrees with the de Gennes theory[19] based on the Ginsburg criterion.

Angular dependences of Γ_B and Γ_C in equations (8) and (9) do not conflict with the observation that at temperatures very near to T_c, Γ_s appears to show the k^2-dependence as well as Γ_f.

Concentration dependence of dynamic properties

Figures 11 and *12* show concentration dependence of Γ_f and Γ_s at the Θ-temperature along with $\bar{\Gamma}$ for the dilute solution. $\bar{\Gamma}$ is continuously connected with Γ_f and has the minimum value at a concentration around 0.02–0.03 g per gram, while Γ_s is a decreasing function of concentration. In *Figure 13* the concentration dependence of A_s/A_f at the Θ-temperature is shown. The ratio A_s/A_f is larger the nearer to C_c the concentration is. Similar concentration dependence of A_s/A_f was also observed at temperatures below Θ. This tendency is enhanced as the temperature approaches T_c.

It is thought that the fast and slow modes observed in semidilute solutions are related to the cooperative motion of entangled chains, i.e. the pseudo-gel motion, and to the translational diffusion of a single chain, i.e. the reptation motion, respectively[5–7,9–13].

Concentration dependence of Γ for the gel-mode at the Θ-temperature is predicted as[12]

$$\Gamma_{gel}\ (\text{at } \Theta) \propto 1/\xi \propto C \tag{12}$$

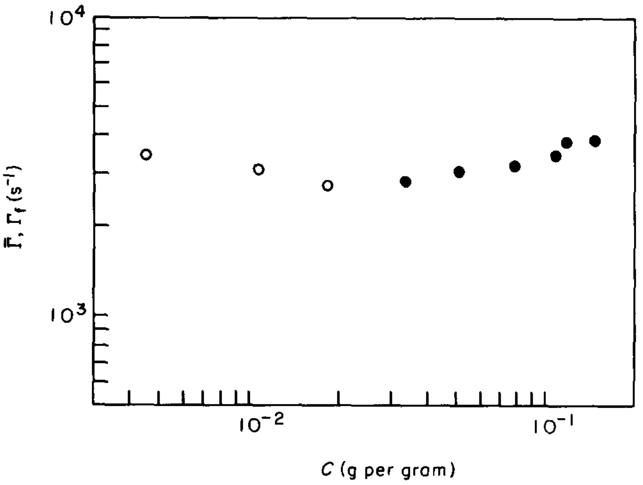

Figure 11 Concentration dependence of Γ_f (●) and $\bar{\Gamma}$ (○) at the Θ-temperature measured at $\theta=90°$ and $\lambda_0=633$ nm

The value of Γ_f slightly increases with increasing concentration, in qualitative agreement with equation (12). However, the slope of the log Γ_f vs. log C plot does not reach unity, and no concentration region such that a simple power-law relation holds was found in this experiment. Amis *et al.*[12] and Brown *et al.*[10] assigned the fast mode to the gel-mode, but found a weak C-dependence of Γ_f similar to our result, i.e. D_c $(=\Gamma_f/k^2)\propto C^{0-0.5}$ (Amis *et al.*) *and* $D_c \propto C^{0.46}$ (Brown *et al.*). The power law of equation (12) should hold in a more concentrated region, if it holds at all. The temperature dependences of slow and fast modes for the critical solution have suggested that Γ_s rather than Γ_f varies in proportion to $1/\xi$ (see previous section). Near C_c or overlap concentration C^*, however, assigning the observed modes to the pseudo-gel mode or the reptation motion may be meaningless, because the correlation length ξ and the radius of gyration R_g are of the same order in this concentration region, and the two motions are essentially indistinguishable.

The line-width of the reptation motion is predicted to have the following scaled form in the semidilute region[12]

$$\Gamma_{\text{rept}} \sim N^{-2}C^{-3} \tag{13}$$

Γ_s (*Figure 12*) shows a stronger concentration dependence than the prediction of equation (13) at higher concentrations. Furthermore, it does not show the k^2-dependence (section on correlation function profile). Hence, it may be concluded that Γ_s does not correspond directly to the diffusion coefficient of a single chain. Actually, it has been found in good solvent systems that the diffusion coefficient for the slow mode ($D_s = \Gamma_s/k^2$) was one or two orders of magnitude smaller than the diffusion coefficient of a single chain measured by pulsed-field gradient n.m.r. and forced Rayleigh scattering[7,20]

For Θ-solvent systems, Amis *et al.*[12] have observed the concentration dependence of $\Gamma_s \propto N^{-2}C^{-3}$ in good agreement with equation (13), while Brown *et al.*[10] have found almost no dependence of Γ_s on C. Since dynamic light scattering of semidilute theta solution has not been studied so extensively as yet, more experimental investigations are needed to obtain the consistent interpretation for the origin of the slow mode.

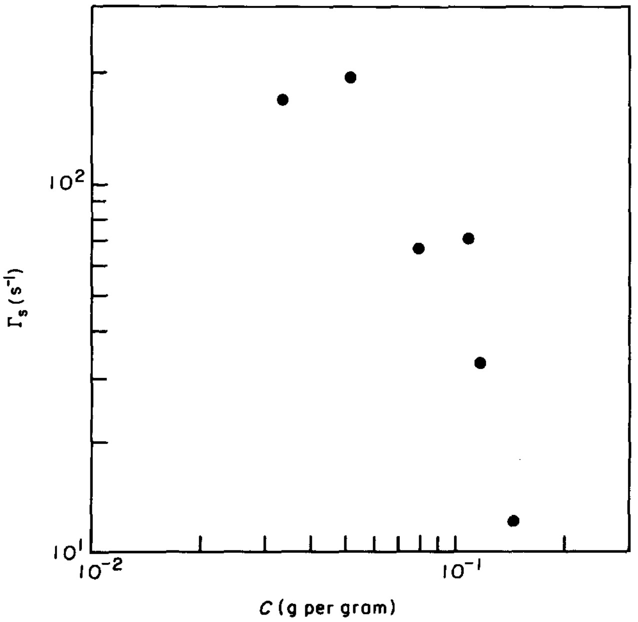

Figure 12 Concentration dependence of Γ_s at the Θ-temperature measured at $\theta = 90°$ and $\lambda_0 = 633$ nm

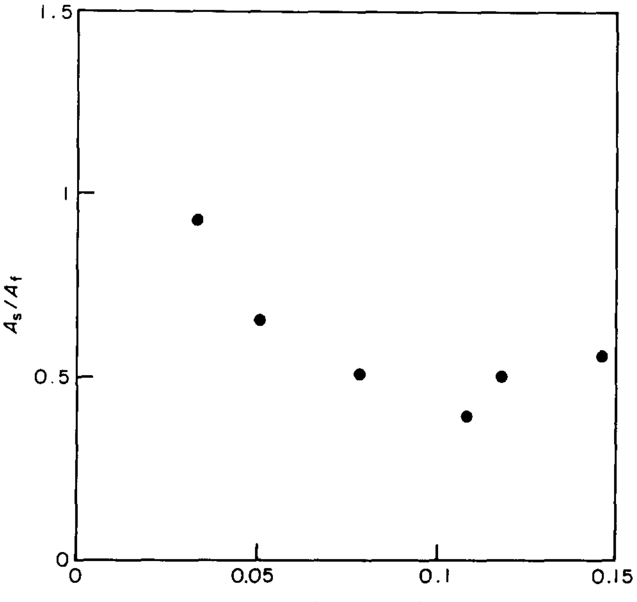

Figure 13 Concentration dependence of A_s/A_f at the Θ-temperature measured at $\theta = 90°$, and $\lambda_0 = 633$ nm

The theoretical explanation of the bimodal decay in semidilute theta solution was presented by Brochard and de Gennes[21,22]. The anomalous angular dependence of Γ_s observed here appears to be explained as the case of $\rho\Gamma_{\text{gel}}T_r > 1$ in their theory, where ρ is the ratio of elastic modulus to isothermal osmotic rigidity and T_r is the reptation time. However, the concentration dependences predicted by the theory, $\Gamma_f \sim C^0$ and $\Gamma_s \sim C^{-2}$, are not consistent with our experimental results.

APPENDIX

The diffusion equation[23] for concentration fluctuations of a binary fluid mixture is given by

$$\frac{\partial C(r)}{\partial t} = -\operatorname{div} J(r) \quad J(r) = (-L/k_BT)\nabla\mu(r) \tag{A1}$$

where $C(r)$, L and $\mu(r)$ are the local concentration, the Onsager kinetic coefficient and the chemical potential density, respectively. For the evaluation of $\mu(r)$, we adopt the Flory–Huggins-type free energy[23,24]

$$F/k_BT = \int_V \left\{ \frac{C(r)}{N}\ln C(r) + (1-C(r))\ln(1-C(r)) + \chi C(r)(1-C(r)) + \frac{a^2}{36C(r)}(\nabla C(r))^2 \right\} dV \tag{A2}$$

where the integration should be made over all space. The chemical potential density $\mu(r)$ is derived by taking the variation of equation (A2) as

$$\mu(r)/k_BT = N^{-1}\ln C(r) - \ln(1-C(r)) + N^{-1} - 1 + \chi(1-2C(r)) - \frac{a^2}{18C(r)}\nabla^2 C(r) + \frac{a^2}{36C(r)^2}(\nabla C(r))^2 \tag{A3}$$

Neglecting the last term in equation (A3)[25], and defining $\delta C(r)$ as the deviation of concentration from an equilibrium concentration C, i.e. $C(r)=C+\delta C(r)$, we can obtain the diffusion equation of $\delta C(r)$ from equations (A1) and (A3) as

$$\frac{\partial \delta C(r)}{\partial t}=L\left((\nabla^2\delta C(r))\{N^{-1}C^{-1}+(1-C)^{-1}-2\chi\}-\frac{a^2}{18C}\nabla^2(\nabla^2\delta C(r))\right) \tag{A4}$$

The Fourier transform of equation (A4) yields Γ_B as

$$\Gamma_B=-\frac{1}{\delta C_k}\frac{\partial \delta C_k}{\partial t}=k^2L\left(N^{-1}C^{-1}+(1-C)^{-1}-2\chi+\frac{a^2k^2}{18C}\right) \tag{A5}$$

The critical concentration C_c and critical temperature χ_c expressed in terms of χ are given[26] by

$$C_c=(1+N^{1/2})^{-1}$$

and

$$\chi_c=\tfrac{1}{2}(1+N^{1/2})^2/N$$

The requirement that Γ_B of the critical solution in the hydrodynamic region ($k\xi<1$) at the Θ-temperature should be described by

$$\Gamma_B/k^2\sim k_BT/(6\pi\eta_sR_g)=k_BT/(6\pi\eta_saN^{1/2})$$

because of $C_c\sim C^*$ (ref. 27), allows us to put

$$L\sim k_BT/(12\pi\eta_sa)$$

Then, finally, we have the expression

$$\Gamma_B\sim k^2\frac{k_BT}{12\pi\eta_sa}\left(\frac{\chi_c-\chi}{\chi_c}\right)(1+k^2\xi^2) \tag{A6}$$

with the correlation length

$$\xi=(1/18)^{\frac{1}{2}}N^{1/4}a\left(\frac{\chi_c-\chi}{\chi_c}\right)^{-1/2} \tag{A7}$$

In the hydrodynamic region, Γ_B is given by

$$\Gamma_B\sim k^2\frac{k_BT}{\eta_sa}\left(\frac{\chi_c-\chi}{\chi_c}\right) \tag{A8}$$

On the other hand, the critical part Γ_C in the hydrodynamic region is given by

$$\Gamma_C=k^2\frac{k_BT}{6\pi\eta^*\xi}=\frac{k_BT}{2^{1/2}\pi\eta^*N^{1/4}a}\left(\frac{\chi_c-\chi}{\chi_c}\right)^{1/2} \tag{A9}$$

from the Kawasaki theory equation (1) and equation (A7). The present treatment is the classical one, resulting in the classical critical exponents.

REFERENCES

1 Takahashi, M. and Nose, T. *Polym. J.* 1984, **16**, 771
2 Kawasaki, K. *Ann. Phys.* 1970, **61**, 1
3 Munch, J. P., Candau, S., Herz, J. and Hild, G. *J. Phys.* 1977, **38**, 971
4 Mathiez, P., Mouttet, C. and Weisbuch, G. *J. Phys.* 1980, **41**, 519
5 Yu, T. L., Reihanian, H. and Jamieson, A. M. *Macromolecules* 1980, **13**, 1590
6 Amis, E. J. and Han, C. C. *Polymer* 1982, **23**, 1403
7 Brown, W., Stilbs, P. and Johnsen, R. M. *J. Polym. Sci., Polym. Phys. Edn.* 1983, **21**, 1029; Brown, W., Johnsen, R. M. and Stilbs, P. *Polym. Bull.* 1983, **9**, 305; Brown, W. *Macromolecules* 1984, **17**, 66
8 Selser, J. C. *J. Chem. Phys.* 1983, **79**, 1044
9 Eisele, M. and Burchard, W. *Macromolecules* 1984, **17**, 1636
10 Brown, W. and Johnsen, R. M. *Macromolecules* 1985, **18**, 379
11 Chu, B. and Nose, T. *Macromolecules* 1979, **12**, 599; ibid. 1980, **13**, 122
12 Amis, E. J., Han, C. C. and Matsushita, Y. *Polymer* 1984, **25**, 650
13 Adam, M. and Delsanti, M. *J. Phys. Lett.* 1984, **45**, L-279
14 Munch, J. P., Hild, G. and Candau, S. *Macromolecules* 1983, **16**, 71
15 Koppel, D. E. *J. Chem. Phys.* 1972, **57**, 4814
16 Stanley, H. E. 'Introduction to Phase Transitions and Critical Phenomena', Clarendon Press, Oxford, 1971, ch. 10, p. 170
17 Swinney, H. L. and Henry, D. L. *Phys. Rev.* 1973, **A8**, 2586
18 Oxtoby, D. W. and Gelbart, W. M. *J. Chem. Phys.* 1974, **6**, 2957
19 De Gennes, P. G. *J. Phys. Lett.* 1977, **38**, L-441
20 Chang, T. and Yu, H. *Macromolecules* 1984, **17**, 115
21 Brochard, F. and De Gennes, P. G. *Macromolecules* 1977, **10**, 1157
22 Brochard, F. *J. Phys.* 1983, **44**, 39
23 De Gennes, P. G. *J. Chem. Phys.* 1980, **72**, 4756
24 Nose, T. *Polym. J.* 1975, **8**, 96
25 Binder, K. *J. Chem. Phys.* 1983, **79**, 6387
26 Shultz, A. R. and Flory, P. J. *J. Am. Chem. Soc.* 1952, **74**, 4760
27 De Gennes, P. G. 'Scaling Concepts in Polymer Physics', Cornell University Press, Ithaca, N.Y., 1979, ch. IV, p. 115